Chapter 9

Exfoliated Nanocomposites Based on Polyaniline and Tungsten Disulfide

Barrit C.S. Lane , Rabin Bissessur ,
Alaa S. Abd-El-Aziz , Wael H. Alsaedi ,
Douglas C. Dahn , Emma McDermott and
Andrew Martin

Additional information is available at the end of the chapter

http://dx.doi.org/10.5772/63457

Abstract

Nanocomposite materials consisting of polyaniline (PANI) and exfoliated WS_2 were synthesized. The WS_2 was prepared by reacting tungstic acid with thiourea at 500°C under nitrogen flow. Samples were prepared with a WS_2 content of 1, 5, 7.5, 10, 12.5, 15, 20, 37, and 64% by mass. An improvement in the electronic conductivity value of the PANI was observed through the incorporation of exfoliated WS_2. The electronic conductivity of PANI-15%WS_2 was 24.5 S/cm, an eightfold increase when compared to pure PANI. Powder X-ray diffraction (XRD), transmission electron microscopy (TEM) and electron paramagnetic resonance (EPR) provided evidence that the nanocomposites are in an exfoliated state. XRD and TEM showed that the nanocomposites were completely amorphous, suggesting lack of structural order in these materials, while their EPR signals were considerably narrower compared to pure PANI, indicating the formation of genuine exfoliated systems. Furthermore, our research showed that WS_2 can be used as a filler to improve activation energy of decomposition of the polymer. By using the Ozawa method, we studied the decomposition kinetics for the nanocomposites, as well as for the pure polymer. The activation energy for the decomposition of pure PANI was found to be 131.2 kJ/mol. Increasing the amount of WS_2 to 12.5% in the PANI increases the activation energy of decomposition to 165.4 kJ/mol, an enhancement of 34.2 kJ/mol over the pure polymer.

Keywords: nanocomposite, polyaniline, transition metal dichalcogenide, exfoliated systems, graphene analogous material

1. Introduction

There has recently been a significant amount of interest concerning the development of a wide variety of inorganic-polymer-based nanocomposite materials. The preparation of these nanocomposites involves the incorporation of various inorganic nanoparticles into the matrix of a certain polymer using methods such as sol-gel processing, blending or mixing the polymer and filler material, as well as *in situ* polymerization [1]. A variety of different nanoparticles including clays, metal oxides, transition metal dichalcogenides (TMDs) and semiconductor metallic crystals have been incorporated into polymeric materials. The resulting nanocomposites typically exhibit improved properties derived from the presence of both the polymer and filler material. Depending on the polymer and the filler material, the improved properties synergistically derived from the two components may include enhancement in thermal stability, electrical conductivity and mechanical strength.

Graphene is a material that has attracted a tremendous amount of interest in the scientific community. It is an allotrope of carbon prepared by exfoliation of graphite into individual two-dimensional layers. Interest in graphene arises from the fact that it possesses a number of unique electrical, thermal, and mechanical properties due to its two-dimensional hexagonal structure [2]. Since the discovery of graphene, much effort has been placed into other layered materials that can be exfoliated into individual sheets in a similar fashion to graphite. One of the most widely studied class of graphite analogues are the transition metal dichalcogenides (TMDs) such as MoS_2, WS_2, $MoSe_2$ and WSe_2. These layered materials possess hexagonal lattice structures that can be exfoliated into single layers, similar to graphite. Due to its ease of exfoliation, MoS_2 has become the most researched TMD for its use in a variety of devices. However, it is interesting to note that WS_2 is much harder to exfoliate, although it is structurally similar to MoS_2. The challenge with the exfoliation of WS_2 has inspired many researchers to examine other methods of exfoliation. Recently, Matte et al. prepared WS_2 nanosheets in an exfoliated state by grinding tungstic acid with an excess of thiourea and heating the reaction mixture to 500°C in an inert atmosphere.

Since the discovery of its conductive nature, polyaniline (PANI) has been one of the most extensively studied electronically conductive polymers for a number of reasons, such as its relative ease of synthesis, low cost of production, high conductivity and impressive environmental stability [3, 4]. Due to these reasons, PANI is considered to be the most promising conductive polymer when compared to others such as polypyrrole, polythiophene and polyacetylene [4]. Over the past 30 years, PANI has become a material of great importance due to its many applications such as in rechargeable batteries, microwave and radar devices, nonlinear optical and light-emitting devices, sensors, catalysts and solar cells [5–12]. In this chapter, we discuss the synthesis of exfoliated WS_2 and the preparation of inorganic-polymer nanocomposites through the incorporation of WS_2 into the polymer matrix of PANI via an *in situ* polymerization technique. Characterization of the exfoliated WS_2 and PANI-WS_2 nanocomposites is also discussed.

1.1. Polyaniline

Polyaniline (PANI) is among the most widely studied polymeric materials due to its electronically conductive nature. The discovery of PANI can be traced back almost 200 years to the experiments of Runge, who reported a colour change from dark green to black upon heating a mixture of copper(II) chloride and aniline nitrate [13]. Although the existence of this polymer has been known for quite some time, it was not until over 100 years after its discovery that PANI was shown to demonstrate significant electrical conductivity [14].

Generally speaking, the synthesis of PANI can be achieved using two different methods: chemical polymerization and electrochemical polymerization. The chemical synthesis of PANI involves the polymerization of aniline using strong oxidizing agents in acidic media. The electrochemical polymerization of PANI can be carried out in a one compartment cell or a two compartment cell in an aqueous medium or a suitable solvent [15]. It has been reported that PANI synthesized using the electropolymerization method results in a sample with lower conductivity, lower crystallinity, higher solubility, and higher bandgap energy when compared to the chemically synthesized polymer [4]. Although it is apparent that there are some advantages associated with the electrochemical synthesis of PANI, the chemical polymerization method is favoured for the large scale production of the polymer [15].

Most frequently, the oxidants used in the chemical synthesis of PANI include ammonium peroxydisulfate (APS) and Fe(III) compounds; however, a wide variety of oxidizing agents have recently been employed. These oxidizing agents include a number of different transition metal compounds such as Mn(III), Mn(IV), Cr(VI), V(V) and Cu(II). Other reported oxidants include KIO_3, H_2O_2 and benzoyl peroxide [16]. There have been many reports on the chemical synthesis of PANI; however, the use of APS in its preparation typically results in the highest electrical conductivity [17].

Depending on the type of oxidizing agent and the reaction conditions, there are two fundamentally different ways that aniline can be oxidized. If the oxidizing agent has a high oxidation potential and does not possess a reactive oxygen atom, it is able to remove electrons or hydrogen from the aniline monomer which results in the formation of dianilines in reduced and/or oxidized form, oxidatively cyclized dianiline products, as well as linear/branched aniline oligomers and PANI. Oxidizing agents with a reactive oxygen atom are able to either donate the oxygen to the aniline monomer resulting in the formation of oxygen-containing products, and/or remove electrons/hydrogen from the aniline monomer [16]. There are a number of oxidants which can act as either oxygen donors or electron acceptors depending on the reaction conditions. In the case of oxygen donor species, high temperatures and alkaline conditions result in the formation of favourable products. However, the opposite is true for the electron acceptor mechanism, where low temperatures and acidic conditions produce favourable results. Peroxydisulfate salts such as APS are able to either donate oxygen or accept electrons; however, the latter is the preferred mechanism for the production of PANI. The reaction of APS with aniline in alkaline conditions at an elevated temperature prompts the donation of oxygen by the APS which results in the production of insoluble oxygen-/sulphur-containing oligoanilines, whereas the same reaction in acidic conditions at a low temperature

leads to the production of PANI as the major product through acceptance of electrons by APS [14].

PANI exists in four different forms depending on the level of oxidation of the polymer. The fully reduced form of the polymer is known as leucoemeraldine, the half oxidized form is referred to as the emeraldine base, and the fully oxidized form is pernigraniline. Although PANI is known to be a conductive polymer, all of these three forms are insulating. The conductive nature of PANI arises only when it is in the emeraldine salt form, where repeating units of the completely oxidized form are followed by units of the completely reduced form [14]. When doped with HCl, PANI demonstrates a significant increase in conductivity by approximately 10 orders of magnitude. Although this mechanism is not entirely understood, it has been proposed that protonation of the emeraldine base of the polymer leads to a spinless bipolaron structure, which rearranges and splits into two polaron units resulting in the emeraldine salt form [18].

1.2. Transition metal dichalcogenides

Graphene has gained significant attention over the past number of years due to its incredible properties. Research into 2D graphene has led to the award of the Nobel Prize in Physics in 2010. Graphene possesses unique electrical, thermal, and mechanical properties and is widely researched for its potential applications in different devices [2]. The unique properties of graphene are due to its two-dimensional hexagonal structure. The discovery of graphene has triggered a considerable amount of interest in other materials that possess layered structures that can be exfoliated into single layers.

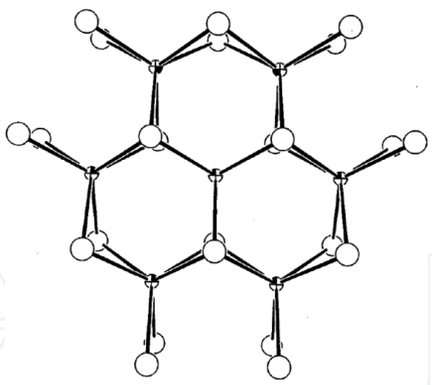

Figure 1. Structure of graphene analogue WS_2.

Layered materials that have recently been studied include TMDs, BC_3, silicene, transition metal carbides and nitrides, and a number of coordination polymers, each of which exists in a structure composed of stacked layers analogous to graphite [19]. These graphite analogues can be cleaved into single layers that are more or less structurally similar to that of graphene. Among these graphene analogous materials, the TMDs are among the most widely studied. Similar to graphene, they possess a two-dimensional hexagonal 'honey-comb' like lattice structure as shown in **Figure 1**. These materials are composed of a transition metal that is

covalently sandwiched between two chalcogen atoms which make up the two-dimensional layer. Weak van der Waals forces exist between the two-dimensional sheets of the TMDs and are responsible for the layered structure of the materials.

There are approximately 60 different TMDs, 40 of which exist in the layered form [20]. Variations in the compositions of TMDs result in a variety of different properties possessed by the compound. TMDs can exist in three different forms which are a result of altering the transition metal or the chalcogen (S, Se, Te) causing changes in the coordination or oxidation state of the material. These forms include metallic, semimetallic and semiconductor. For example, $NbSe_2$ is a metallic material, whereas WS_2 is semiconducting [21].

Out of the many TMDs, those containing a group six transition metal are among the most highly researched. Recently, MoS_2 as well as the chemically similar WS_2 have been materials of interest due to the fact that they are layered semiconductors with tunable bandgaps depending on size [22, 23]. Much like graphene, these materials possess unique properties when in an exfoliated state. Due to its ease of exfoliation, MoS_2 has been the more highly researched TMD for its use in a variety of devices.

There are a number of methods for preparing exfoliated MoS_2, the most common being exfoliation by the n-butyllithium technique [24]. First, the bulk MoS_2 is mixed with an n-butyllithium/hexane solution in order to achieve lithium-intercalation. The Li_xMoS_2 is then submerged in water, resulting in the production of LiOH and the evolution of H_2 gas causes separation of the MoS_2 layers.

Although WS_2 is similar in chemical structure to MoS_2, exfoliation of WS_2 using the n-butyllithium technique is much more difficult [25, 26]. This difficulty arises from the fact that when WS_2 is mixed with the n-butyllithium hexane solution, very little lithium intercalation occurs. When performing lithiation of MoS_2, the resulting Li_xMoS_2 typically has a lithium content of $x \approx 1$. WS_2 under identical conditions yields Li_xWS_2, with an x value of under 0.4. As a result, there is negligible H_2 formation when Li_xWS_2 is submerged in water causing the degree of WS_2 exfoliation to be very low [26]. Consequently, this has inspired researchers to examine other methods of WS_2 exfoliation. A solvothermal method has been used to increase the amount of lithium intercalation in WS_2 [27]. Other reported methods include using a strong acid treatment to separate the WS_2 layers, as well as using different synthetic techniques to prepare the WS_2 in an already exfoliated state [28–30].

Recently, Wu et al. reported a method of preparing WS_2 nanosheets in an exfoliated state. This method involved ball-milling WO_3 in the presence of sulphur and heating to 500–800°C under argon atmosphere [29]. Shortly after, Matte et al. reported a method for the preparation of exfoliated WS_2 which involved the use of thiourea as the source of sulphur and tungstic acid as the source of tungsten. This process simply involves grinding of tungstic acid with an excess of thiourea (tungstic acid–thiourea 1:48 mole ratio), and heating the mixture to 500°C under nitrogen atmosphere [30].

Once in an exfoliated state, WS_2 has a wide variety of potential applications including photoconductors, catalysts, lubricants and lithium batteries [29]. Although there are many potential

applications for this material, the amount of work done on WS_2 has been quite limited compared to other TMDs.

1.3. Inorganic-polymer nanocomposites

There has been significant research into the development of a wide variety of inorganic-polymer-based nanocomposites. Inorganic-polymer nanocomposites are materials that consist of inorganic nanoparticles mixed with a polymer where the size of the inorganic nanoparticle is less than 100 nm, for example layered materials, incorporated into a polymer host [31]. Research into these types of materials is primarily concerned with the enhancement of the polymer properties through the incorporation of different particles with varying characteristics. Examples of polymer properties that are considered include thermal stability, electrical conductivity and mechanical strength. A variety of different nanoparticles such as clays, metal oxides, transition metal dichalcogenides and semiconductor metallic crystals have been previously incorporated into polymeric matrices. There are a number of different methods used to prepare inorganic-polymer nanocomposites such as blending or mixing the polymer and filler material, sol–gel processing, and *in situ* polymerization [1].

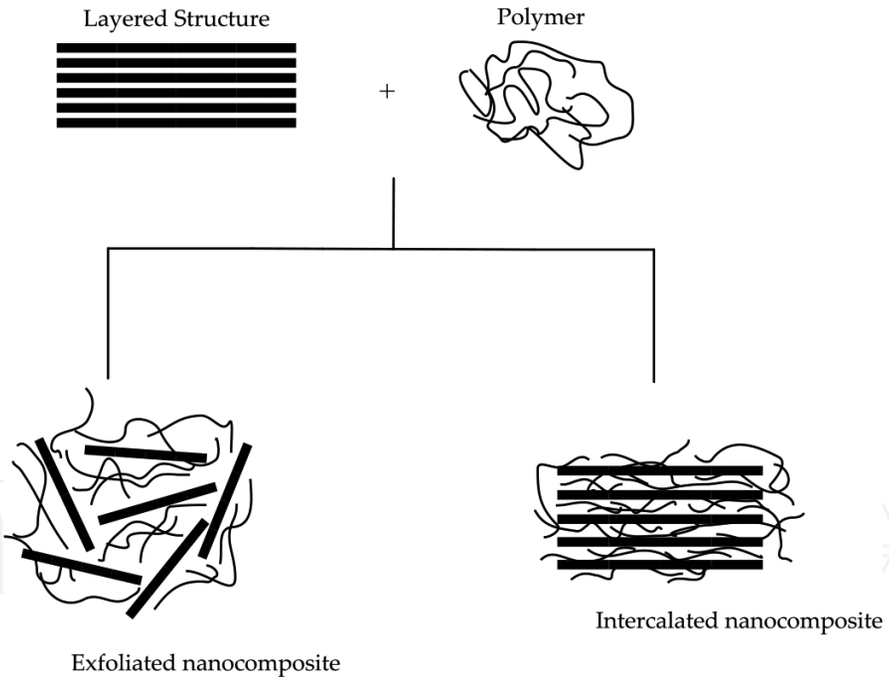

Figure 2. Intercalated and exfoliated nanocomposites.

Polymer-based nanocomposites containing layered materials can exist in two major forms: exfoliated nanocomposites and intercalated nanocomposites (**Figure 2**). Exfoliated nanocomposites consist of single or few layered nanosheets incorporated within a polymer matrix. Conversely, intercalated nanocomposites are materials formed when the layered species are stacked with polymer chains, resulting in alternating inorganic and polymeric layers.

http://dx.doi.org/10.5772/63457

XRD characterization of the nanocomposite is very useful for determining its structural characteristics. In particular, XRD can be used to detect three types of nanocomposites. For an immiscible nanocomposite, the powder pattern is similar to that of the starting layered structure, demonstrating no change in d-spacing, and therefore suggesting that no separation of the layers took place. For an intercalated nanocomposite, its XRD pattern will be different from that of the pristine lamellar structure. Typically, an increase in d-spacing is observed due to the incorporation of the polymer in the gallery spaces of the inorganic host. Finally, in the case of an exfoliated nanocomposite, no peaks are expected in the XRD scan. This is due to the fact that there is no regular spacing between the layers of the material, indicating that the layers are exfoliated and distributed throughout the polymer matrix [31]. It is also worth noting that the XRD scan of the exfoliated nanocomposite assumes that the incorporated polymer is completely amorphous. However, a polymer possessing a crystalline structure could show diffraction peaks in the XRD pattern of its corresponding exfoliated nanocomposite.

2. Synthetic methodology

2.1. Synthesis of exfoliated WS_2

Tungstic acid was purchased from Sigma-Aldrich and used as received. Typical synthesis of exfoliated WS_2 involved grinding and mixing tungstic acid in excess of thiourea with the use of a mortar and pestle. The mole ratio of the tungstic acid to thiourea was 1:48. This mixture was placed in a ceramic reaction vessel and inserted into a ceramic tube installed in a split furnace. The mixture was then heated to approximately 500°C for 3.5 h under nitrogen atmosphere and then allowed to cool overnight under nitrogen purge. This yielded a black solid product which was ground to a fine powder for use in future reactions.

2.2. Synthesis of polyaniline-WS_2 nanocomposites

A sample of distilled aniline along with 1 M HCl was placed in a large Erlenmeyer flask. The solution was placed in an ice bath and cooled to approximately 0°C with mechanical stirring. A sample of the previously synthesized WS_2 was suspended in 10–20 mL of deionized water and probe-sonicated for approximately 20 min at 30% amplitude. The WS_2 suspension was then added to the aniline solution and stirred mechanically while keeping the temperature between 0°C and 5°C.

A solution of ammonium peroxydisulfate (APS) was prepared by dissolving a sample of APS in 1 M HCl. This solution was cooled in an ice bath and then slowly added to the aniline-WS_2 mixture. The mole ratio of aniline to APS was 1:1. The reaction mixture was left to stir for 1.5 h before the product was collected by vacuum filtration, washed thoroughly with 1 M HCl, and left to dry overnight under suction.

For the synthesis of bulk polyaniline, the same procedure as outlined above was used, but without addition of any WS_2.

3. Instrumentation

Powder X-ray diffraction (XRD) was performed using a Bruker AXS D8 Advance instrument equipped with a graphite monochromator, variable divergence slit, variable antiscatter slit and scintillation detector. Cu (Kα) radiation (λ = 1.524 Å) was used for sample measurements carried out at room temperature. Samples were run in air from 2 to 60° (2θ).

Thermogravimetric analysis (TGA) was performed on a TA Instruments TGA Q500 in dry air or nitrogen purge. For measurements performed under nitrogen, the furnace was allowed to purge for 15 min using a 60.00 mL/min purge flow rate before the measurement was started. The heating rates used were varied between 5 and 40°C/min. The range of heating used was from 20 to 800°C.

Scanning electron micrographs were obtained on an LVEM5 benchtop instrument, operating at 5 kV. Powdered samples were placed on carbon-taped stubs prior to analysis.

High-resolution transmission electron microscopy (HRTEM) was performed on a Hitachi 7500 Bio-TEM, using an accelerating voltage of 80 kV. The powdered samples were dispersed in deionized water with the help of ultrasonication, and the dispersed samples were cast on carbon-coated copper grids.

Electrical conductivity measurements were performed using the four-probe van der Pauw technique on a home built system. Samples were prepared as thin circular pressed pellets, 12.7 mm in diameter, with a thickness between 0.5 and 1.0 mm. Pellets were attached to a sample holder with either vacuum grease or double-sided tape, and wires were secured to the pellets using silver or carbon paste. Room-temperature conductivity measurements were performed in air. For some samples, variable-temperature conductivity measurements were also made, with the pellets in vacuum.

EPR spectra were recorded using a Bruker Elexsys E580 pulse spectrometer operating in CW mode. The solid samples were placed in Suprasil EPR sample tubes (4 mm o.d.) and were sealed.

4. Results and discussion

4.1. Characterization of exfoliated WS_2 nanoparticles

In order to determine whether or not the synthesized product was in fact WS_2 in an exfoliated state, powder XRD diffraction data were collected. The diffractogram is shown below in **Figure 3(b)**.

XRD data show that the synthesized WS_2 is highly amorphous in nature, with a low crystallinity percentage of 17.2%, as determined by the XRD software. The diffractogram shows the presence diffraction peaks at approximately 33° (2θ) and 58° (2θ) corresponding to the (100) and the (110) planes, respectively. In contrast, the XRD diffractogram of pristine layered WS_2

http://dx.doi.org/10.5772/63457

(**Figure 3a**), shows the characteristic (002) line just above 14° (2θ). The lack of the (002) line and the presence of the (100) and (110) lines in the diffractogram of the synthesized WS_2 indicate that it is, in fact, in an exfoliated state. The XRD data correlate well with the literature for exfoliated WS_2 synthesized via the n-butyllithium method [25].

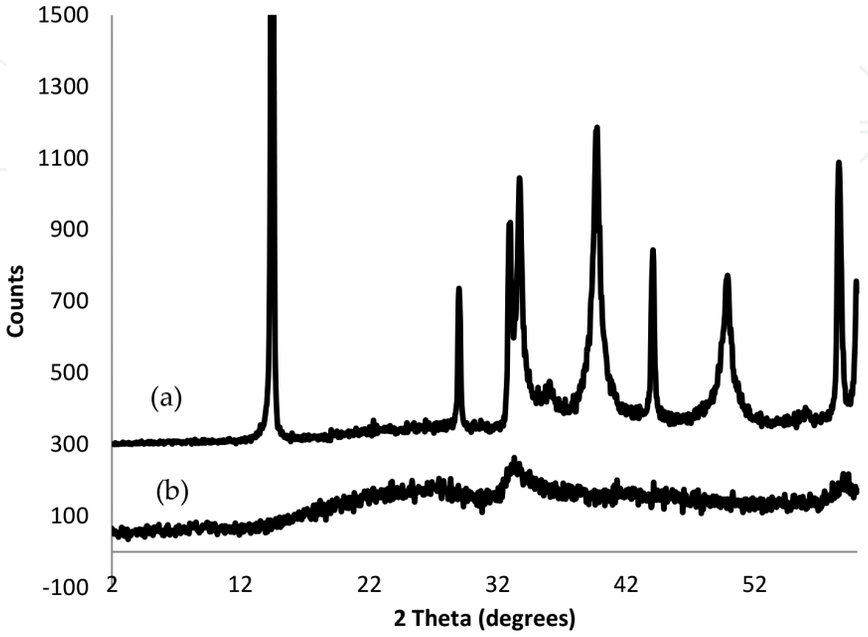

Figure 3. (a) XRD diffractogram of (a) pristine layered WS_2 (Aldrich), (b) synthesized WS_2.

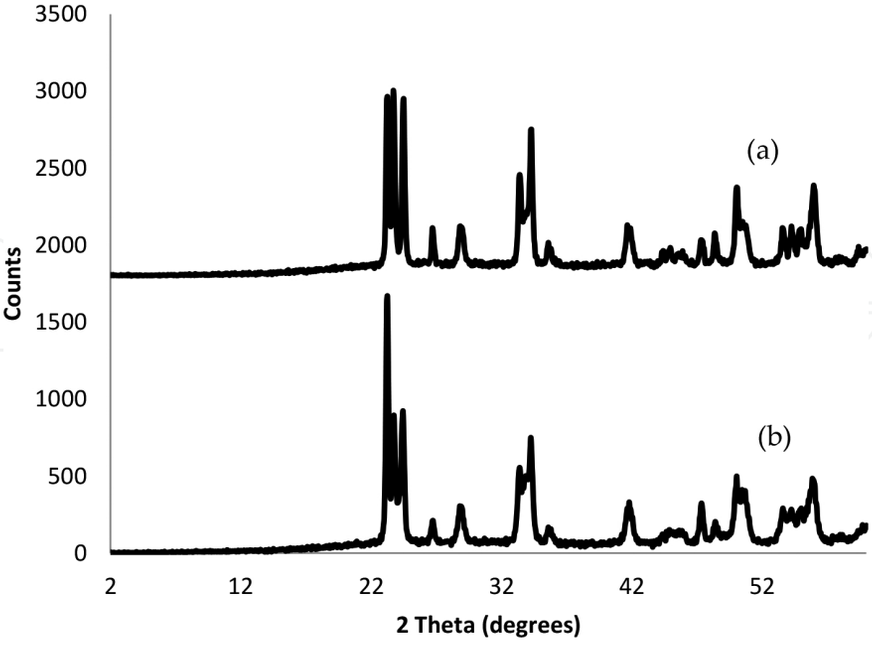

Figure 4. XRD of products obtained after TGA in air: (a) product from synthesized exfoliated sample, (b) product from pristine layered sample.

TGA was performed in air on the synthesized exfoliated WS_2 and on pristine layered WS_2 (Aldrich). Both TGA runs resulted in the formation of a light green powder, demonstrating oxidation of both samples. It was assumed that in both cases, WO_3 was formed as a result of oxidation of the initial materials. To confirm this, XRD data were collected on both light green samples and the results were compared to the literature data for pure WO_3. It was noted that the diffraction peaks shown in both diffractograms (**Figure 4**) correlated well with one another, and closely resembled the literature powder pattern of WO_3 [32]. It was also found that the light green products from exfoliated WS_2 and pristine layered WS_2 demonstrated a similar high percentage in crystallinity of 79.4% and 76.6%, respectively. This confirms that both WS_2 samples were oxidized to WO_3, and thus possess a similar chemical composition.

Electrical conductivity measurements were performed on pressed pellets of the synthesized exfoliated WS_2 using the van der Pauw technique. The synthesized exfoliated WS_2 was found to be non-conductive, while pristine layered WS_2 exhibits a conductivity value of 3.6×10^{-3} S/cm.

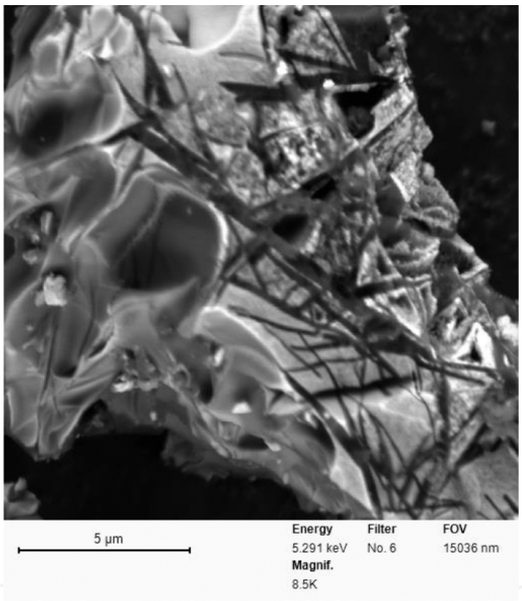

Figure 5. SEM micrograph of exfoliated WS_2.

SEM was performed on the exfoliated WS_2 in order to gain insight into its surface morphology. As shown in the SEM micrograph (**Figure 5**), the material appears to be amorphous, which is consistent with the XRD data.

TEM was used to further characterize the material in order to gain a more in-depth understanding of the structure of the material. As viewed under TEM, exfoliated WS_2 appears to be very thin and membrane like. The membranes do not stack, clearly indicating the disordered state of the material. There is also a certain degree of folding/wrinkling of the membranes. It could also be observed that the exfoliated WS_2 is quite porous, and might potentially have a very large surface area (**Figure 6**).

http://dx.doi.org/10.5772/63457

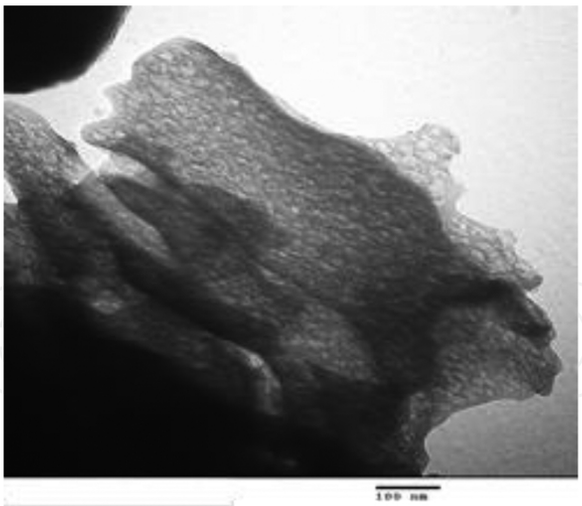

Figure 6. TEM of exfoliated WS_2.

4.2. Characterization of polyaniline

XRD was used to characterize the synthesized PANI. The diffractogram features a very broad peak, indicating a low degree of crystallinity of the material. The XRD analysis software calculated a low percent crystallinity of 11.6%, clearly indicating a highly disordered structure (**Figure 7**). This is consistent with the fact that PANI is an amorphous polymer, and is in agreement with the literature [33].

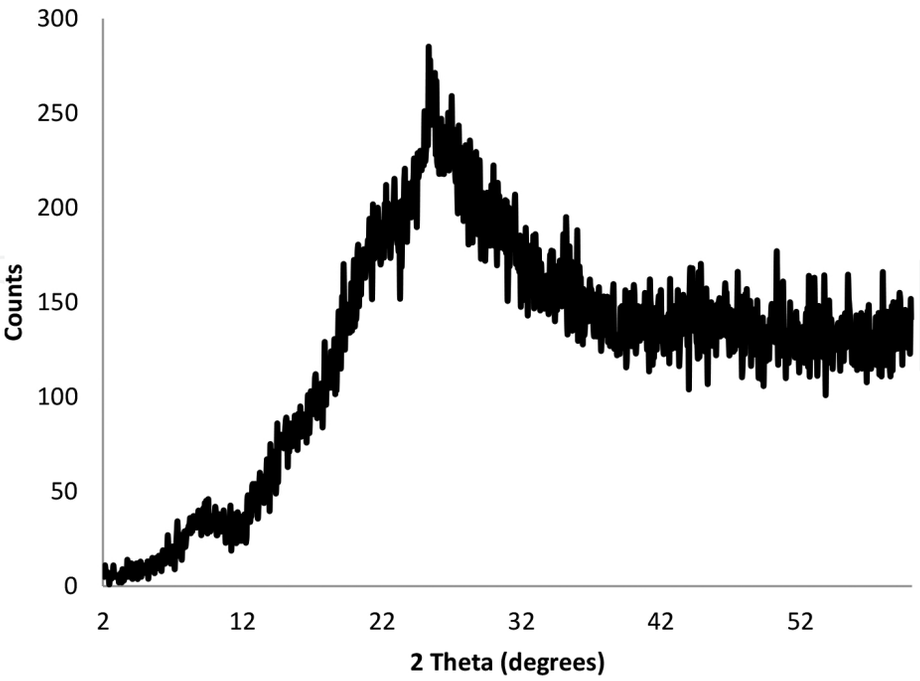

Figure 7. XRD diffractogram of pure PANI.

FTIR was also used to characterize the PANI. The FTIR spectrum correlates well with the literature, demonstrating wavenumbers within the same range [33].

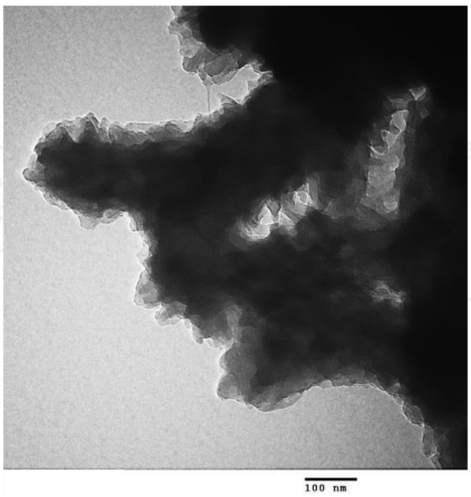

Figure 8. TEM micrograph of bulk PANI.

Electron microscopy was also used to further characterize the bulk PANI. Bulk PANI as observed under SEM and TEM shows that it is completely featureless, and highly disordered. The TEM micrograph of bulk PANI is shown in **Figure 8**.

4.3. XRD characterization of PANI-WS_2 nanocomposites

Powder X-ray diffraction data were collected on the prepared PANI-WS_2 nanocomposites (**Figure 9**).

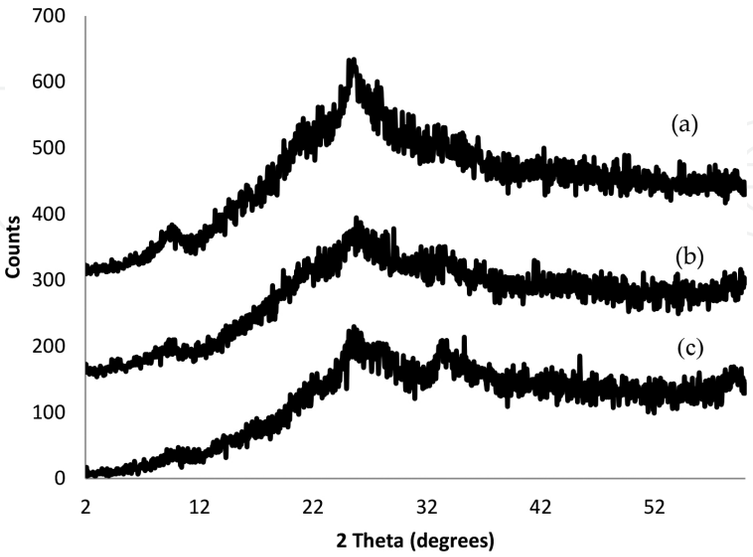

Figure 9. Diffractograms of nanocomposites (a) PANI-10%WS_2, (b) PANI-20%WS_2, (c) PANI-37%WS_2.

XRD data provided evidence for the formation of exfoliated nanocomposites. The XRD scans for all prepared compositions appeared to be highly amorphous and lacked any sharp crystalline peaks, indicating that the materials possessed a low degree of structural order. It was also observed that as the WS_2 content is increased, the appearance of the characteristic exfoliated WS_2 diffraction peaks just above 33° and 58° became more apparent. These peaks were not detected in the XRD scans of samples with lower WS_2 content, which closely resemble the scan of the bulk polymer.

4.4. Transmission electron microscopy on PANI-WS_2 nanocomposites

Transmission electron microscopy was further used to characterize the nanocomposites. All nanocomposites as viewed under TEM showed that they are in a completely amorphous, disordered state, and these findings are in very good agreement with the powder X-ray diffraction data. Thus, TEM further confirms the formation of exfoliated systems. As an illustration, the TEM micrographs of PANI-10%WS_2 and PANI-64%WS_2 are shown in **Figure 10(a)** and **(b)**.

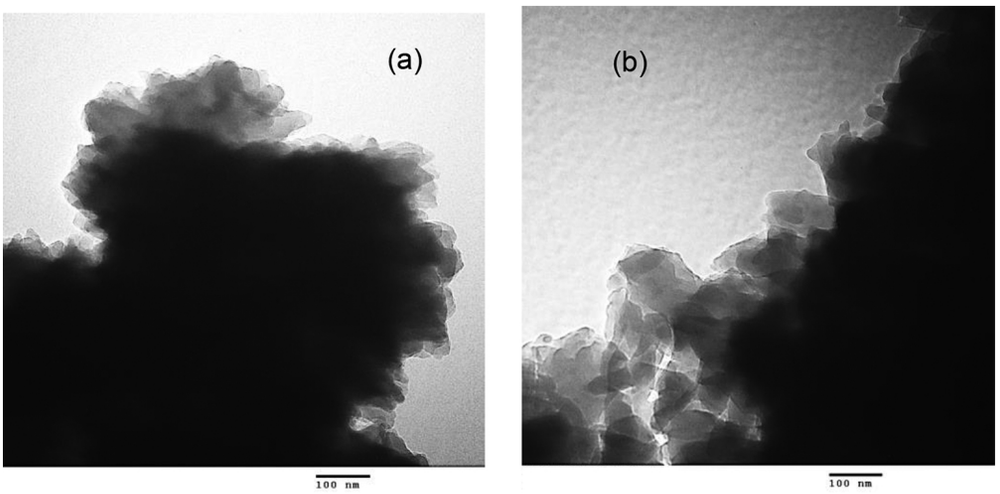

Figure 10. TEM micrographs of (a) PANI-10%WS_2, (b) PANI-64%WS_2.

4.5. EPR analysis of PANI-WS_2 nanocomposites

Electron paramagnetic resonance spectroscopy was used to characterize the PANI-WS_2 nanocomposites, as well as the pure PANI and exfoliated WS_2. As an illustration, the overlaid EPR spectra of pure PANI, exfoliated WS_2 and PANI-20%WS_2 nanocomposite are shown in **Figure 11**. Exfoliated WS_2 was found to be EPR silent, and pure PANI showed an EPR signal with a g-value of 2.0023. However, the PANI-20%WS_2 nanocomposite demonstrated an intense peak that was significantly narrower than that of the pure PANI. The dramatic difference in EPR signal between the pure PANI and that of the PANI-20%WS_2 material implies that the WS_2 and PANI in the nanocomposite are not simply a physical mixture, but are actually mixed at the molecular level. Other compositions showed similar behaviour.

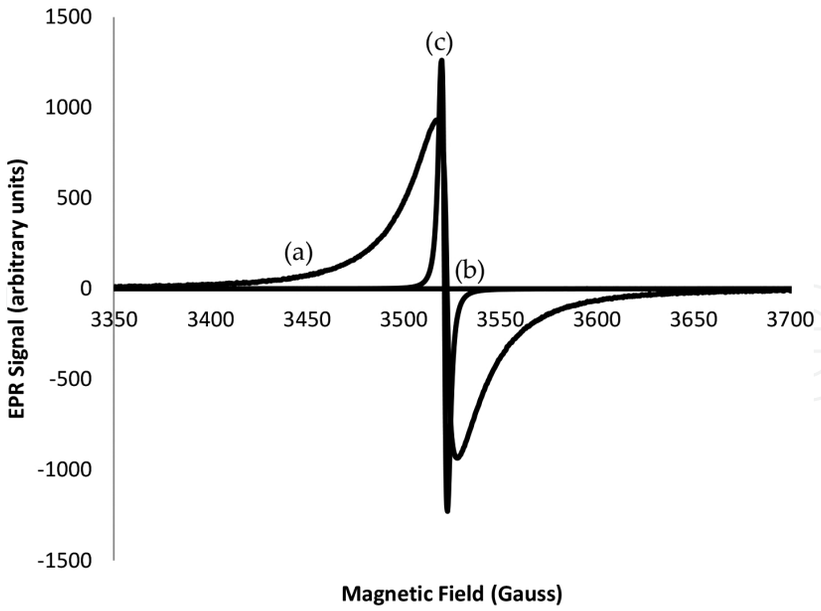

Figure 11. EPR spectra of (a) pure PANI, (b) exfoliated WS_2, and (c) PANI-20%WS_2.

4.6. Decomposition kinetics of PANI-WS_2 nanocomposites

The decomposition kinetics of the PANI-WS_2 nanocomposites (1, 5, 7.5, 10, 12.5, 15, 20, 37 and 64%) and pure PANI were determined using the Ozawa method [34, 35]. The Ozawa method involved performing a series of TGAs at different heating rates (5, 10, 20 and 40°C/min), obtaining the conversion curves from the thermograms, and then a series of Ozawa plots at different conversion values. The activation energy of decompositions (E_a) were then determined from the Ozawa plots. The results are summarized in **Table 1** and displayed in **Figure 12**. The data demonstrate that the presence of WS_2 in PANI enhances its activation energy of decomposition. The maximum enhancement (about 34 kJ/mol) was observed at 12.5% by mass of WS_2.

% by mass of WS_2	E_a (kJ/mol)	Standard deviations (kJ/mol)
0	131.2	±7.7
1	146.6	±5.1
5	133.1	±9.3
7.5	133.2	±15.9
10	152.3	±4.8
12.5	165.4	±5.5
15	151.2	±5.2
20	129.5	±8.4
37	144.8	±12.7
64	152.5	±11.5

Table 1. Activation energies of PANI-WS_2 nanocomposite samples.

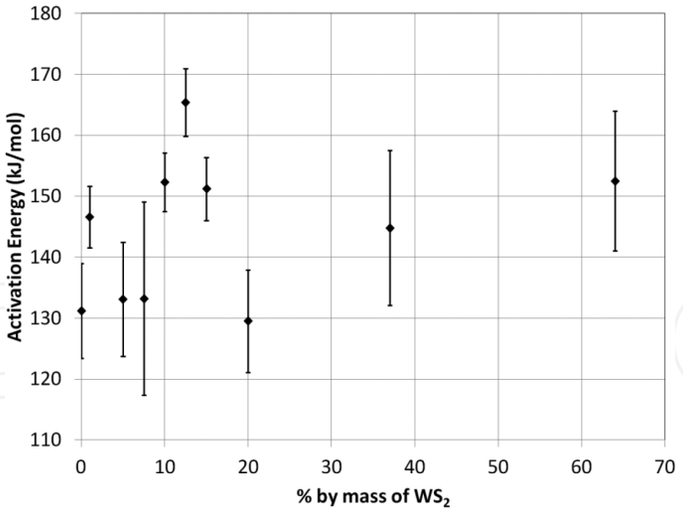

Figure 12. Plot of activation energy values versus mass% of WS_2.

4.7. Electrical conductivity of PANI-WS_2 nanocomposites

Room temperature conductivity values for the nanocomposite samples are summarized below in **Table 2**, and plotted in **Figure 13**. The accuracy of the conductivity of a given sample is about ±10%. For some of the nanocomposite compositions, several pellets were measured and each conductivity value is listed. Considerable variation is observed in some cases, but this is not surprising considering that the samples were pellets made from pressed powders. Conductivity can be affected many factors such as the pressure used in forming the pellets, the quality of inter-grain contact, sample aging, and the humidity of the air. In addition, different batches of PANI may have slightly different oxidation or doping levels.

WS_2 content in nanocomposite	Room-temperature conductivity (S/cm)
0% (Pure PANI)	3.1, 3.7, 5.0, 5.3
1%	0.60, 0.68
5%	0.022, 0.024, 0.051
7.5%	0.30
10%	13
12.5%	8.8, 16
15%	24, 25
20%	9.1
37%	8.5, 10
64%	8.0

Table 2. Nanocomposite conductivity at room temperature. Multiple values indicate readings on different samples of the same nominal composition.

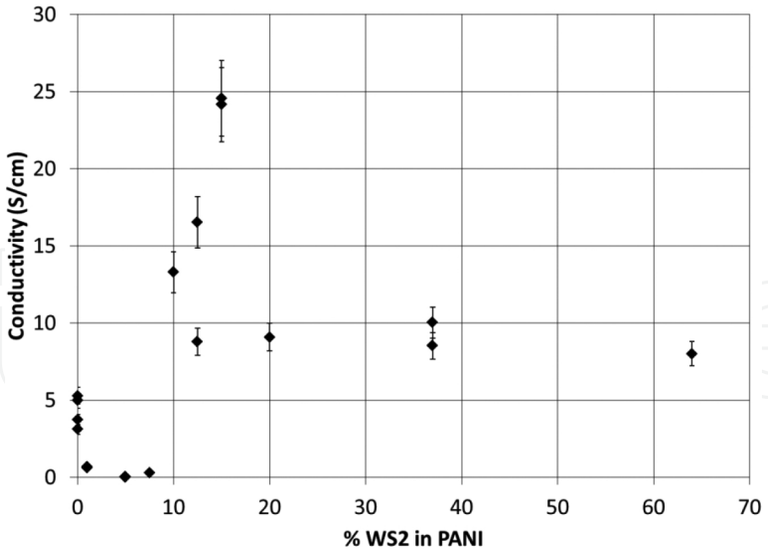

Figure 13. Nanocomposite conductivity at room temperature.

Two pellets of exfoliated WS_2 were tested but showed no detectable conductivity. WS_2 is known to be a semiconductor, and when a pellet pressed from bulk WS_2 powder (Aldrich) was measured a conductivity of 3.6×10^{-3} S/cm was found. We conclude that either our exfoliated WS_2 is much less conducting than bulk WS_2, or that the inter-grain contact in our pellets of exfoliated WS_2 is so poor as effectively prevent conduction through the pellet.

As seen in **Table 2** and **Figure 13**, as the percentage of WS_2 in the nanocomposites is increased, the conductivity drops initially, reaching a minimum at about 5% by mass. This drop is not surprising, since we are adding poorly-conducting WS_2 to conducting PANI. However, as the percentage of WS_2 is increased further, the conductivity rises again, and samples containing at least 10% WS_2 demonstrate a significant enhancement in electronic conductivity over the pure polymer. The 15% samples exhibited the highest electronic conductivity at about 24 S/cm. When a two-component composite material is more conducting than either of its components, this suggests that interaction between the components has altered the electrical properties of one or both of the components. For example, a layered nanocomposite consisting of polypropylaniline intercalated between layers of FeOCl was a much better conductor than either FeOCl or polypropylaniline alone [36]. This is believed to be due to electron transfer from the polymer to the FeOCl layers. The nature of the interaction causing conductivity enhancement in the PANI/WS_2 system above 10% WS_2 is not yet understood, and will be a topic for future research.

Variable-temperature conductivity measurements were attempted on a number of the samples. In the experimental system used, the sample is in vacuum and can be cooled to 50 K or below. The pressed pellet nanocomposite samples were quite fragile and often cracked on exposure to vacuum or due to thermal stresses on cooling. For this reason, it was only possible to obtain variable-temperature data on the pure PANI, as well as 12.5% and 20% WS_2–PANI nanocomposite samples. The results are shown in **Figure 14**.

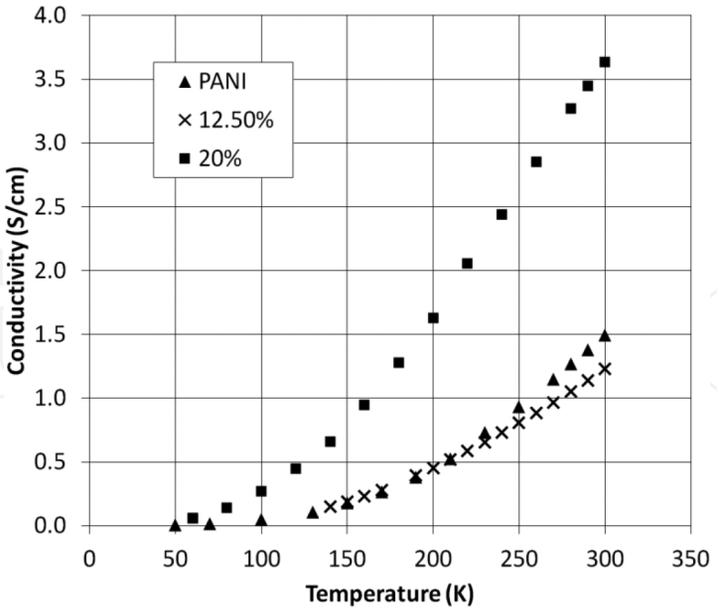

Figure 14. Variable temperature conductivity of PANI, PANI-12.5%WS_2 nanocomposite, and PANI-20%WS_2 nanocomposite.

It was also observed that conductivity dropped when the pellets were placed in vacuum, possibly due to the loss of small amounts of residual water. For example, the PANI sample shown in **Figure 14** had a conductivity of 3.1 S/cm in air. This dropped to 2.0 S/cm after 4 h in vacuum at room temperature, and to 1.5 S/cm after 24 h. After this, the variable-temperature measurements were made, and then the sample was returned to air for four days, after which the conductivity was 2.9 S/cm, close to the original value. Similar conductivity decreases in vacuum were observed in the nanocomposite samples, especially the 12.5% sample, which was in vacuum for a longer time than the others.

The variable-temperature data are consistent with the variable-range hopping (VRH or Mott law) model for conduction in disordered materials. In the VRH model, the resistivity ρ is given as a function of absolute temperature T by

$$\rho(T) = \rho_0 \, exp\left[\left(\frac{T_0}{T}\right)^{\frac{1}{d+1}} \right] \tag{1}$$

where d is the dimensionality of the material, and T_0 and ρ_0 are parameters that are nearly independent of temperature. Both three-dimensional and two-dimensional Mott law behaviours have been reported in a number of studies of conducting polymer and nanocomposite systems [36–38]. If Eq. (1) with d = 3 is valid, a plot of ln ρ as a function of $T^{-1/4}$will be linear. Our data are plotted in this format in **Figure 15**. The straight-line behaviour seen in the figure shows that the three-dimensional VRH model is a reasonable description of electrical conduction in these materials.

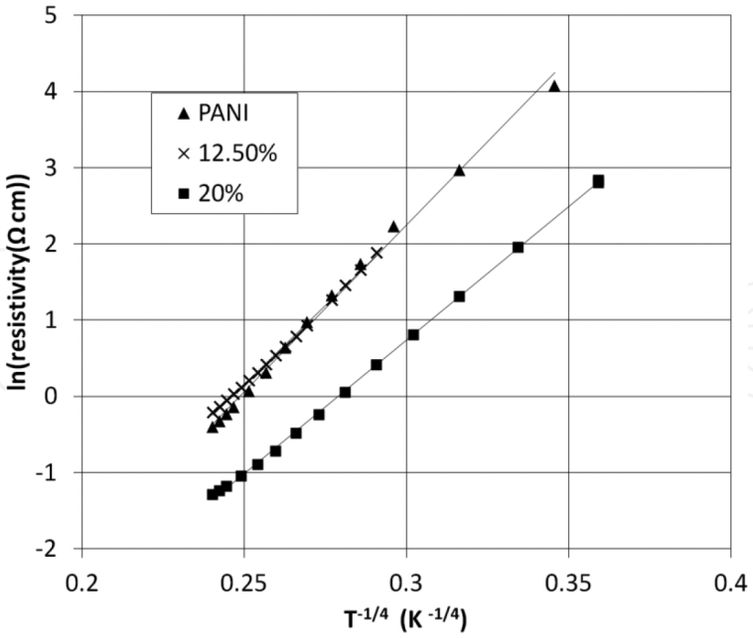

Figure 15. Three-dimensional VRH model of PANI, PANI-12.5%WS_2 nanocomposite, and PANI-20%WS_2 nanocomposite.

If $d = 2$ in Eq. (1) a plot of ln ρ as a function of $T^{-1/3}$will be linear. Our data also appears nearly linear in such a plot, and the 12.5% data with its more limited temperature range even appears nearly linear in a plot of ln ρ as a function of $T^{-1/2}$(d = 1). We conclude that our variable-temperature conductivity data are consistent with VRH conduction, although the dimensionality d cannot be determined precisely.

5. Conclusion

A significant amount of information was generated on the synthesized PANI-WS_2 nanocomposite materials. Evidence has been provided to show that the WS_2 synthesized from thiourea and tungstic acid is in an exfoliated state. XRD, TEM and EPR provide evidence that genuine exfoliated nanocomposites have been prepared through the incorporation of the exfoliated WS_2 into PANI. Furthermore, the incorporation of exfoliated WS_2 into PANI resulted in significant changes in the thermal and electrical properties of the polymer.

Acknowledgements

Financial support was provided by the Natural Sciences and Engineering Research Council of Canada (NSERC) and the University of Prince Edward Island is gratefully acknowledged. We thank Professor Art van der Est (Chemistry Department, Brock University) for collecting the EPR data.

Author details

Barrit C.S. Lane[1], Rabin Bissessur[1*], Alaa S. Abd-El-Aziz[1], Wael H. Alsaedi[1], Douglas C. Dahn[2], Emma McDermott[1] and Andrew Martin[2]

*Address all correspondence to: rabissessur@upei.ca

1 Department of Chemistry, University of Prince Edward Island, Charlottetown, Prince Edward Island, Canada

2 Department of Physics, University of Prince Edward Island, Charlottetown, Prince Edward Island, Canada

References

[1] Haldorai Y, Shim J-J, Lim KT. Synthesis of Polymer-Inorganic Filler Nanocomposites in Supercritical CO_2. Journal of Supercritical Fluids. 2012; 71: 45–63. doi:10.1016/j.supflu.2012.07.007.

[2] Singh V, Joung D, Zhai L, Das S, Khondaker SI, Seal S. Graphene Based Materials: Past, Present and Future. Progress in Materials Science. 2011; 56: 1178–1271. doi:10.1016/j.pmatsci.2011.03.003.

[3] Stejskal J, Gilbert RG. Polyaniline. Preparation of a Conducting Polymer (IUPAC Technical Report). Pure and Applied Chemistry. 2002; 74: 857–867. doi:10.1351/pac200274050857.

[4] Bhadra S, Singha NK, Khastgir D. Electrochemical Synthesis of Polyaniline and its Comparison with Chemically Synthesized Polyaniline. Journal of Applied Polymer Science. 2007; 104: 1900–1904. doi:10.1002/app.

[5] MacDiarmid AG, Yang LS, Huang WS, Humphrey BD. Polyaniline: Electrochemistry and Application to Rechargeable Batteries. Synthetic Metals. 1989; 18: 393–398. doi: 10.1016/0379-6779(87)90911-8.

[6] de Chanterac H, Roduit P, Belhadj-Tahar N, Fourrier-Lamer A, Djigo Y, Aeiyach S, Lacaze PC. Electromagnetic Absorption of Polyanilines at Microwave Frequencies. Synthetic Metals. 1992; 52: 183–192. doi: 10.1016/0379-6779(92)90306-4.

[7] Mäkelä T, Sten J, Hujanen A, Isotalo H. High Frequency Polyaniline Shields. Synthetic Metals. 1999; 101: 707. doi:10.1016/S0379-6779(98)01095-9.

[8] Halvorson C, Cao Y, Moses D, Heeger AJ. Third Order Nonlinear Optical Susceptibility of Polyaniline. Synthetic Metals.1993; 57: 3941-3944. doi: 10.1016/0379-6779(93)90538-8.

[9] Wang HL, MacDiarmid AG, Wang YZ, Gebier DD, Epstein AJ. Application of Polyaniline (Emeraldine Base, EB) in Polymer Light-Emitting Devices. Synthetic Metals. 1996; 78: 33–37. doi:10.1016/0379-6779(95)03569-6.

[10] Dutta D, Sarma TK, Chowdhury D, Chattopadhyay A. A Polyaniline-Containing Filter Paper that Acts as a Sensor, Acid, Base, and Endpoint Indicator and Also Filters Acids and Bases. Journal of Colloid and Interface Science. 2005; 283: 153–159. doi:10.1016/j.jcis.2004.08.051.

[11] Drelinkiewicz A, Waksmundzka-Gòra A, Sobczak, JW, Stejskal J. Hydrogenation of 2-ethyl-9, 10-anthraquinone on Pd-polyaniline(SiO_2) Composite Catalyst: The Effect of Humidity. Applied Catalysis A: General. 2007; 333: 219. doi:10.1016/j.apcata.2007.09.011.

[12] Chang M-Y, Wu C-S, Chen Y-F, Hsieh B-Z, Huang W-Y, Ho K-S, Hsieh T-H, Han Y-K. Polymer Solar Cells Incorporating One-Dimensional Polyaniline Nanotubes. Organic Electronics. 2008; 9: 1136–1139. doi:10.1016/j.orgel.2008.08.001.

[13] Runge von FF. Ueber einige Produkte der Steinkholendestillation. Annalen der Physik Und Chemie. 1834; 107: 65–78. doi:10.1002/andp.18341070502.

[14] Macdiarmid AG, Chiang JC, Richter AF, Epstein AJ. Polyaniline: A New Concept in Conducting Polymers. Synthetic Metals. 1987; 18: 285–290. doi: 10.1016/0379-6779(87)90893-9.

[15] Marie E, Rothe R, Antonietti M, Landfester K. Synthesis of Polyaniline Particles via Inverse and Direct Miniemulsion. Macromolecules. 2003; 36: 3967–3973. doi:10.1021/ma0257550.

[16] Ćirić-Marjanović G. Recent Advances in Polyaniline Research: Polymerization Mechanisms, Structural Aspects, Properties and Applications. Synthetic Metals. 2013; 177: 1–47. doi:10.1016/j.synthmet.2013.06.004.

[17] Gök A, Sarı B, Talu M. Synthesis and Characterization of Conducting Substituted Polyanilines. Synthetic Metals. 2004; 142: 41–48. doi:10.1016/j.synthmet.2003.07.002

[18] Varela-Álvarez A, Sordo JA. A Suitable Model for Emeraldine Salt. Journal of Chemical Physics. 2008; 128: 174706-1–174706-6. doi:10.1063/1.2913246.

[19] Tang Q, Zhou Z. Graphene-Analogous Low-Dimensional Materials. Progress in Materials Science. 2013; 58: 1244–1315. doi:10.1016/j.pmatsci.2013.04.003.

[20] Wilson JA, Yoffe AD. The Transition Metal Dichalcogenides Discussion and Interpretation of the Observed Optical, Electrical and Structural Properties. Advances in Physics. 1969; 18: 193–335. doi:10.1080/00018736900101307.

[21] Ibrahem MA, Lan T-w, Huang JK, Chen Y-Y, Wei K-H, Li L-J, Chu CW. High Quantity and Quality Few-Layers Transition Metal Disulfide Nanosheets from Wet-Milling Exfoliation. RSC Advances. 2013; 3: 13193–13202. doi:10.1039/c3ra41744a.

[22] Mak KF, Lee C, Hone J, Shan J, Heinz TF. Atomically Thin MoS_2: A New Direct-Gap Semiconductor. Physical Review Letters. 2010; 105: 136805-1–136805-4. doi:10.1103/PhysRevLett.105.136805.

[23] Albe K, Klein A. Density-Functional-Theory Calculations of Electronic Band Structure of Single-Crystal and Single-Layer WS_2. Physical Review B. 2002; 66: 073413-1–073413-3. doi:10.1103/PhysRevB.66.073413.

[24] Xu B-H, Lin B-Z, Sun D-Y, Ding C. Preparation and Electrical Conductivity of Polyethers/WS_2 Layered Nanocomposites. Electrochimica Acta. 2007; 52: 3028–3034. doi:10.1016/j.electacta.2006.09.046.

[25] Miremadi BK, Morrison SR. The Intercalation and Exfoliation of Tungsten Disulfude. Journal of Applied Physics. 1988; 63: 4970–4974. doi:10.1063/1.340441.

[26] Yang D, Frindt RF. Li-Intercalation and Exfoliation of WS_2. Journal of Physics and Chemistry of Solids. 1996; 57: 1113–1116. doi:10.1016/0022-3697(95)00406-8.

[27] Xu B-H, Lin B-Z, Chen Z-J, Li X-L, Wang Q-Q. Preparation and Electrical Conductivity of Polypyrrole/WS_2 Layered Nanocomposites. Journal of Colloid and Interface Science. 2009; 330: 220–226. doi:10.1016/j.jcis.2008.10.033.

[28] Bhandavat R, David L, Singh G. Synthesis of Surface-Functionalized WS_2 Nanosheets and Performance as Li-Ion Battery Anodes. Journal of Physical Chemistry Letters. 2012; 3 (11): 1523–1530. doi:10.1021/jz300480w.

[29] Wu Z, Wang D, Zan X, Sun A. Synthesis of WS_2 Nanosheets By a Novel Mechanical Activation Method. Materials Letters. 2010; 64: 856–858. doi:10.1016/j.matlet.2010.01.040.

[30] Ramakrishna Matte HSS, Gomathi A, Manna AK, Late DJ, Datta R, Pati SK, Rao CNR. MoS_2 and WS_2 Analogues of Graphene. Angewandte Chemie International Edition. 2010; 122: 4153–4156. doi:10.1002/anie.201000009.

[31] Paul DR, Robeson LM. Polymer Nanotechnology: Nanocomposites. Polymer. 2008; 49: 3187–3204. doi:10.1016/j.polymer.2008.04.017.

[32] Leghari SAK, Sajjad S, Zhang J. A Time Saving and Cost Effective Route for Metal Oxides Activation. RSC Advances. 2014; 4: 5248–5253. doi:10.1039/c3ra46518g.

[33] Xu H, Bissessur R, Dahn DC. Nanomaterials Based on Polyanilines and $MoSe_2$. Journal of Inorganic and Organometallic Polymers and Materials. 2014; 24: 219–225. doi:10.1007/s10904-013-9981-z.

[34] Ozawa, T. Kinetic Analysis of Derivatives Curves in Thermal Analysis. Journal of Thermal Analysis 1970; 2: 301–324. doi:10.1007/BF01911411.

[35] Scully K, Bissessur R. Decomposition Kinetics of Nylon-6/Graphite and Nylon-6/Graphite Oxide Composites. Thermochimica Acta 2009; 490:32–36. doi:10.1016/j.tca.2009.01.029.

[36] Scully SF, Bissessur R, Dahn DC, Xie G. In Situ Polymerization/Intercalation of Substituted Anilines into Iron (III) Oxychloride. Solid State Ionics. 2010; 181: 933–938. doi:10.1016/j.ssi2010.05.015.

[37] Kanatzidis MG, Marcy HO, McCarthy WJ, Kannewurf CR, Marks TJ. In Situ Intercalative Polymerization Chemistry of FeOCl. Generation and Properties of Novel, Highly Conductive Inorganic/Organic Polymer Microlaminates. Solid State Ionics. 1989; 32–33: 594–608. doi:10.1016/0167-2738(89)90272-5.

[38] Reghu M, Cao Y, Moses D, Heeger AJ. Counterion-Induced Processibility of Polyaniline: Transport at the Metal-Insulator Boundary. Physical Review B. 1993; 47: 1758–1764. doi:10.1103/PhysRevB.47.1758.